

UNCLASSIFIED

Defense Technical Information Center
Compilation Part Notice

ADP012268

TITLE: Computational Modeling for Magnetic-Sensor-Based
Three-Dimensional Visualization of Microcracks

DISTRIBUTION: Approved for public release, distribution unlimited

This paper is part of the following report:

TITLE: Applications of Ferromagnetic and Optical Materials, Storage and
Magnetoelectronics: Symposia Held in San Francisco, California, U.S.A. on
April 16-20, 2001

To order the complete compilation report, use: ADA402512

The component part is provided here to allow users access to individually authored sections
of proceedings, annals, symposia, etc. However, the component should be considered within
the context of the overall compilation report and not as a stand-alone technical report.

The following component part numbers comprise the compilation report:
ADP012260 thru ADP012329

UNCLASSIFIED

Computational Modeling For Magnetic-Sensor-Based Three-Dimensional Visualization Of Microcracks

Leonid Muratov, David Lederman, and Bernard R. Cooper
West Virginia University, Morgantown, WV 26506-6315

ABSTRACT

The presence of cracks, phase segregation, or even submicron-sized grain boundaries creates a disruption of the magnetic field response to an externally applied electrical current running through the material. These effects can be detected through the magnetic field leakage in the external near-surface region. Using a computer model of an array of magnetic tunnel junction detectors, magnetic "signatures" of various faults and/or material borders and domains have been calculated using finite element analysis and portrayed by icons. We have considered a number of typical cracks and flaws, of different dimensions and orientations, within the bulk of the component. The database of "signatures" thus generated allows fast recognition of faults and generation of their images in real time. Significant efforts have been made to provide an adequate three-dimensional visualization of the shape and distribution of microcracks, the magnetic field lines, and delineation of the position of the faults in relation to the surface.

INTRODUCTION

A major problem in aircraft maintenance is the effect of wear and tear on major components. For example, cracks emanating from bolt holes on structural components or turbine blades, located below the surface, appear after years of use. These cracks can cause catastrophic damage if they are not detected sufficiently early. Non-destructive evaluation (NDE) and identification (NDI) methods allow early detection of subsurface cracks and corrosion, so that the damaged components can be replaced or repaired. Current methods used for NDE have difficulties in detecting very small cracks, on the order of a tenth of a millimeter or less, which form below the surface.

Our approach consists of fabricating an array of magnetic transistor detectors. The advantage of having an array over a single detector is that the magnetic leakage can be detected simultaneously at different points in space. By modeling the signals from all of the array components simultaneously (a generalized sort of triangulation), it is possible to obtain a three-dimensional image of the cracks and faults. This work focuses on a "proof of concept", and considers the possibility of detecting a small fringing magnetic field originating from faults and distinguishing among different types of faults.

MAGNETIC TUNNEL JUNCTION DETECTOR

Magnetic tunneling junction (MTJ) technology is applicable to the present problem because of its great sensitivity in probing the magnetic response of the metallic components to an applied current. If the material is completely homogenous, the resulting magnetic signal is also homogenous. However, in the presence of phase segregation, cracks, or even submicron-sized grain boundaries, there is a disruption of the normal magnetic flux pattern of the material, causing a leakage field to appear.¹ This field usually has strong gradients that can be detected with these sensitive magnetic sensors.

The sensor used for NDI must be able to map the fringing magnetic fields due to cracks and other faults inside metals. This information can be used by a computer model to recreate a three-dimensional image of faults. The principle of this approach was recently tested using an array of conventional copper microloop pickup coils to detect cracks inside the walls of metal ducts in

nuclear reactors.² MTJ's provide a fundamental advantage with respect to this conventional technology in that their bandwidth of operation is much greater, they operate at much lower frequencies, and their sensitivity is greater. MTJ's also provide a way of measuring the direction and magnitude of the in-plane leakage field, because the magnitude of the conductance in each MTJ is proportional to $(1 - \cos\theta)$, where θ is the angle between the magnetization vectors of the two ferromagnetic layers.³ MTJ's are also superior to giant magnetoresistance (GMR) sensor technology for fabricating sensor arrays. Normally, GMR sensors are operated with the current flowing in the plane of the film; otherwise, the resistivity is too low and difficult to measure. This geometry makes the measurement of individual array components almost impossible to make. In contrast, MTJ sensors have a much lower conductivity, making the measurement of each component possible.

The array of MTJ detectors can be fabricated using standard photolithographic techniques. A sketch of such an array is shown in Fig. 1. Each of the MTJ's composing the array provides a local measure of the magnitude and direction of the magnetic field.

MTJ's are composed of two ferromagnetic, metallic layers separated by an insulating, non-magnetic layer. As current is driven from one ferromagnetic layer to the other, where one of the

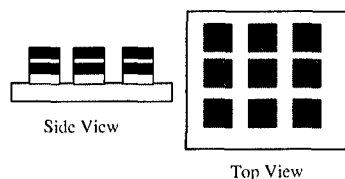


Figure 1 Side and top views of a 3 by 3 MTJ detector array. In reality, the array would have many more elements.

layers acts as an electron spin polarizer, whereas the other acts as an analyzer. The tunneling probability between these two layers is strongly dependent on the relative orientations of the magnetizations of the layers.⁴ It is necessary to pin the magnetization of the polarizer, whereas the analyzer magnetization must rotate easily in small magnetic fields. This can be done by using the phenomenon of exchange bias, where an antiferromagnetic layer is deposited next to the polarizer, hence pinning its magnetization³.

As mentioned above, it is imperative that the direction of the magnetic leakage field as well as its magnitude is known. This can be achieved if the MTJ response is linear, non-hysteretic, and sensitive to small fields. Biasing the unpinned ferromagnetic layer with a dc field at 90° to the pinned layer can do this.⁵

MEASUREMENTS

In order to examine an aircraft component (a sample undergoing NDE) for the presence of faults, a magnetic field should be introduced into the system. For paramagnetic materials, such as aluminum and most superalloys used in engines, an externally applied electrical current can be used to generate the magnetic field. Suppose that the area where the electrical current exists is much smaller than the characteristic size of the sample undergoing NDE. In this case, the magnetic field depends only on the properties of the material being scanned below the measuring tool (array of MTJ's), and does not depend on the shape of the sample or on the position of the measuring tool on the top surface of the component. Therefore, this magnetic field can be compen-

sated by applying an external magnetic field in such a way that, in a fault free environment, the resulting magnetic field is zero at the location of the MTJ sensors.

If there is a fault in the sample, a deviation of the current flowing through the sample will cause a distortion of the magnetic field. The magnitude of the fringing flux will be proportional to the signal measured by each detector, and the shape of the leakage field will depend on the shape of the fault. (Note that sensors can measure only a component parallel to the magnetization of the pinned layer. Rotating the detector by 90° would yield the other component.) Because the detector is composed of an array of MTJ's, a two-dimensional image of the flux lines can be obtained. The applied current can also be rotated by 90° to provide in-plane resolution. In order to improve the depth profiling capabilities, the distance between the detector and the sample can be varied by mounting the array on a precision x - y - z stage.

COMPUTATIONAL MODELING

In order to calculate the magnetic response produced by a fault one needs to know the electrical current inside and outside this fault, including its boundaries. For simplicity, we assume that there is no electrical current inside a crack and that it has simple, very thin boundaries. A simple estimate can be obtained if the relaxation of the electrical current around the fault is neglected. In this model, one can either set the conductivity tensor in the crack area to zero or equivalently, apply an effective current with magnitude equal to the initial current, but flowing in the opposite direction inside the crack. The fringing field (the deviation of the magnetic field from its initial distribution in a fault free material) is just the magnetic field produced by this effective current.

Considering a uniform current of 1A/mm^2 and using the Biot-Savart law, one can estimate that a $50\text{ }\mu\text{m}$ wide crack, located 2 mm below the surface, will generate a field of $\sim 3\text{ mOe}$ at the surface. An effect of the same magnitude can be also produced by a $100\text{ }\mu\text{m}$ cubic void at the same depth. Because of the high sensitivity of the MTJ detectors, this should translate into a sizeable change in conductivity of approximately $0.1 - 0.5\%$.

The presence of a fault would cause an increase in the current density in the areas surrounding the fault, which in turn produces a screening effect and therefore reduces the resulting fringing magnetic field. Accurate calculations of the magnetic field should include this relaxation of the current flowing around the fault. We used a finite-element (FE) analysis of the current distribution around faults to calculate these effects. In the finite-element approximation, a continuous function of the solution of a partial differential equation is replaced by a sum of piecewise functions, each of them being defined within a small volume (finite element). Since the work of Lord *et al*⁶, the FE analysis of the magnetic flux leakage from various flaws in materials has become an established² technique.

For our purposes, we can further simplify the problem by considering only a dc current, and calculate the redistribution of the electrical current inside material composed of conducting and non-conducting phases. Our calculations were based on FEM software developed at NIST⁷ and available without cost.

The NIST FEM software is designed to compute the linear electrical properties of digital images of random materials. This program takes advantage of the existence of the variational principle for the linear conductivity problem. In order to find an equilibrium distribution of currents in the system, the power (energy dissipation per unit time) is minimized with respect to the voltages at the vertices of the finite elements. An externally applied electrical field is included through the boundary conditions. Only a few modifications to this program were required in or-

der to describe the present problem and to have a convenient interface with the visualization software.

The initial distribution of the electrical current in a fault-free sample depends on the way the current is introduced to the system. The details of the experimental design are not been finalized at this time; therefore, there is no reason to choose a specific configuration of the current. For

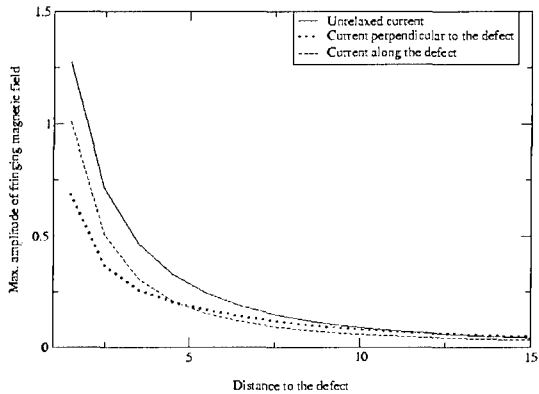


Figure 2. Effect of current relaxation around the fault on the resulting magnetic field. The fault dimensions are 10x1x1 units, it is always parallel to the surface where magnetic field is measured and is placed at various distances from this surface.

simplicity, we have considered a uniform external current. In this configuration, it was found that it is sufficient to consider a relatively small system composed of ~35,000 elements (41x41x21). A calculation of the current takes about one second of the CPU time on AMD Athlon based PC or Compaq Alpha workstation. Test calculations on a much larger system (80x80x40) did not reveal any significant changes.

For the results reported here, the observation plane was always considered at $Z=0$, with the electrical current running along the Y axis. Therefore, the magnetic field has the strongest component (the only component in fault-free environment) in the X direction.

FEM calculations showed that the redistribution of the electrical current plays an important role. For example, when a rod-like crack located close to the surface with a long side perpendicular to the electrical current, the resulting magnetic field is one half of the magnetic field obtained by a simple zeroing of the current inside the crack area (Figure 2). In this geometry, the current that flows around the crack deviates significantly toward the surface where, due to its proximity to the sensor, it contributes significantly to the fringing field. At the same time, when the fault is deep enough, this current is directed mainly toward the surface and it does not contribute to the X projection of the magnetic field measured immediately above the fault (generally, the magnetic response is the strongest at this point), as depicted in Fig. 2. When the same rod-like fault extended parallel to the direction of the current, the relaxation current is much smaller, but it is also extended in the Y direction, and contributes to the X projection of the magnetic field. Therefore, the screening effect is larger when the current is parallel to the longest axis of a deep fault.

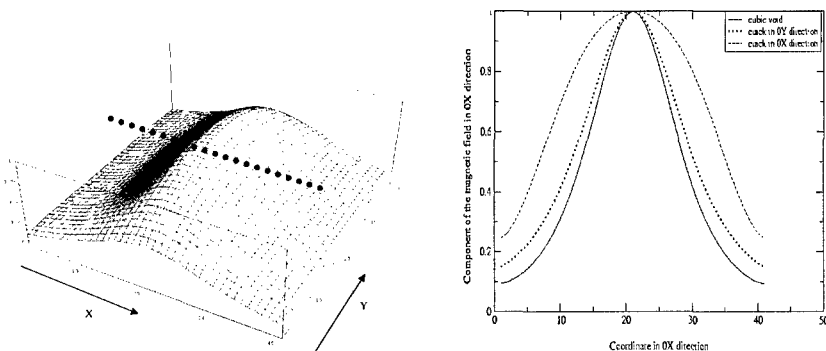


Figure 3. The left panel shows the amplitude of the fringing magnetic field generated by a crack with dimensions of $27 \times 1 \times 1$ units. The crack is located in the center of XY plane, 10 units below the surface and it is extended along Y axis. The right panel shows the amplitudes of the fringing magnetic field generated by a crack when it is parallel and perpendicular to the current and by a cubic void of $3 \times 3 \times 3$ units located at the same depth. The field is calculated using FEM along the dotted line as is shown in the left panel. For both panels, the external current is running in Y direction.

Information about the shape of the fault can be extracted from the 2-d profile of the magnetic field. For simplicity, we first discuss the measurements along two lines on top of an extended rod-like fault. The change in the X component of the magnetic field along the line perpendicular to the applied current and located on top of the center of this modeled crack is shown on Figure 3. When the long axis of the fault is parallel to the current, the measured magnetic field looks similar, but not identical to the response from a cubic void of the same volume (see Fig. 3). When the fault is extended in the direction perpendicular to the current (this can be achieved by rotating the MTJ array and the source of the current), the measured profile looks much different (dashed line on the Fig.3). The fact that magnetic response depends on the mutual orientation of the electrical current and the fault can be used to determine the fault orientation.

The length of the fault that generated profiles shown on Fig. 3 is large in comparison with the distance from the fault to the surface. When the fault is buried deep below the surface (as is the one used for Figs. 2 and 4), measurements that are more extensive are required. However, even in this case, the fringing magnetic field is still dependent on the angle between the current and the long axis of the fault. This is illustrated in Fig. 4, which is a 2-D map of the fringing field (much like the one that would be measured by the MTJ sensor), and shows the large difference between the two configurations.

Knowledge of the magnetic field on the surface of the volume containing a complex fault is not sufficient to uniquely determine the exact shape of the fault. Therefore, empirical information about faults should be used. For example, we can assume that a simple crack can be described by six parameters: three dimensions, two orientation angles, and the depth from the surface. These parameters can be found using a least-squares fit of the calculated to the measured

magnetic fields. The initial guess about the shape of the structure (is it a simple crack or not) can be made by comparing the measured pattern to a library of “signatures” of possible and common faults. We plan to consider a variety of possible faults that will include both cracks and flaws, of different dimensions and orientations, within the bulk of the component. In addition, we will treat faults introduced by such items as bolts and screws (e.g., mini-cracks around bolt holes).

Even a simple two-dimensional figure, such as Fig. 4, is difficult to present on paper or on a flat computer screen. A mutual orientation of a surface of the sample, array of detectors and faults is extremely difficult to depict in an understandable way. Considering a characteristic size of faults $\sim 100 \text{ } \mu\text{m}$ and a detector size 0.5 mm , then in a sample of several centimeters long, many faults could be detected. In order to understand their relative positions, it is necessary to

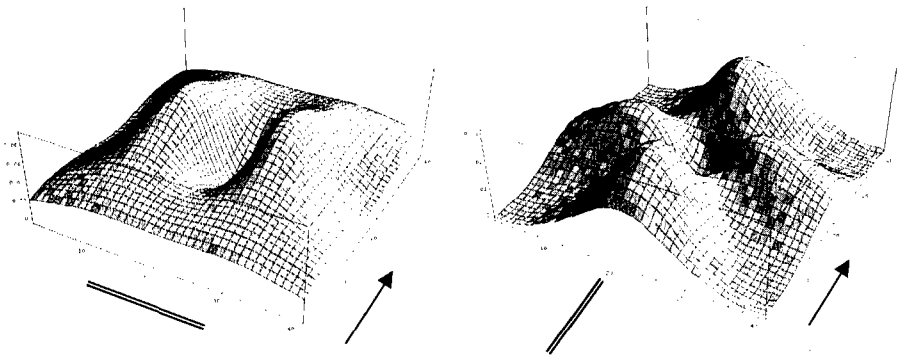


Figure 4. Magnetic signature of the rod-like crack with dimensions $10 \times 1 \times 1$ units parallel to the surface and located 10 units below the surface. The height of plots is related to the in-plane component of the magnetic field perpendicular to the external current. In order to illuminate the differences, a normalized magnetic field generated by the point fault located at the same depth is subtracted from the both plots. An arrow shows the direction of the external current. The double line indicates the orientation of the crack, which is located directly underneath of the centers on the panels.

employ advanced visualization techniques. Volume imaging in three dimensions is the key to our approach. We have adopted a multilayer hierarchy of volume visualization capability. Relatively simple problems are addressed at any location by using inexpensive stereo-ready graphics cards and corresponding eyeware available for PC's. Viewing of complex images at an ImmersaDesk, and/or at a portable CAVE-like system driven by NT or Linux PC can provide a significant increase of viewing quality.

CONCLUSION

Our initial modeling and experimental measurements have shown that it is possible to determine the shape and position of crack-like faults underneath the surface using an array of magnetic tunneling junction detectors. Our simulations showed that a fault located at a depth comparable to its size can be categorized and identified, while faults located deeper can be located, it is more difficult to determine their shapes.

The authors would like to acknowledge the help with computer visualization of faults and magnetic field from the West Virginia University Virtual Environment Laboratory and particularly the assistance from David Baker. This research has been supported by grant F49620-01-J-0315 from AFOSR.

REFERENCES

- ¹ D. Jiles, Magnetism and Magnetic Materials, 2nd Edition (Chapman & Hall, London, 1998).
- ² M. Ueseka, K. Hakuta, K. Miya, K. Aoki, and A. Takahashi, "Eddy-Current Testing by Flexible Microloop Magnetic Sensor Array", IEEE Trans. Magn. 34, 2287 (1998).
- ³ J. S. Moodera, L. R. Kinder, T. M. Wong, and R. Meservey, "Large magnetoresistance at room temperature in ferromagnetic thin film tunnel junctions", Phys. Rev. Lett. 74, 3273 (1995)
- ⁴ M. Julliere, Phys. Lett. 54A 225 (1975).
- ⁵ M. Tondra, J. M. Daughton, D. Wang, R. S. Beech, A. Fink, and J. A. Taylor, J. Appl. Phys. 83, 6688 (1998).
- ⁶ J.Hwang, and W.Lord, Finite Element Modeling Field /Defect Interactions, Journal of Testing and Evaluation 3 (1975) 21-23.
- ⁷ Garboczi, E. J. "Finite Element and Finite Difference Programs for Computing the Linear Electric and Elastic Properties of Digital Images of Random Materials". NISTIR 6269; 211 p. December 1998.